Cancer Research

Tenascin-C Protects Cancer Stem–like Cells from Immune Surveillance by Arresting T-cell Activation

Elena Jachetti[1], Sara Caputo[1,2], Stefania Mazzoleni[3], Chiara Svetlana Brambillasca[1], Sara Martina Parigi[1], Matteo Grioni[1], Ignazio Stefano Piras[4], Umberto Restuccia[5], Arianna Calcinotto[1,5], Massimo Freschi[6], Angela Bachi[5], Rossella Galli[3], and Matteo Bellone[1]

Abstract

Precociously disseminated cancer cells may seed quiescent sites of future metastasis if they can protect themselves from immune surveillance. However, there is little knowledge about how such sites might be achieved. Here, we present evidence that prostate cancer stem–like cells (CSC) can be found in histopathologically negative prostate draining lymph nodes (PDLN) in mice harboring oncogene-driven prostate intraepithelial neoplasia (mPIN). PDLN-derived CSCs were phenotypically and functionally identical to CSC obtained from mPIN lesions, but distinct from CSCs obtained from frank prostate tumors. CSC derived from either PDLN or mPIN used the extracellular matrix protein Tenascin-C (TNC) to inhibit T-cell receptor–dependent T-cell activation, proliferation, and cytokine production. Mechanistically, TNC interacted with α5β1 integrin on the cell surface of T cells, inhibiting reorganization of the actin-based cytoskeleton therein required for proper T-cell activation. CSC from both PDLN and mPIN lesions also expressed CXCR4 and migrated in response to its ligand CXCL12, which was overexpressed in PDLN upon mPIN development. CXCR4 was critical for the development of PDLN-derived CSC, as *in vivo* administration of CXCR4 inhibitors prevented establishment in PDLN of an immunosuppressive microenvironment. Taken together, our work establishes a pivotal role for TNC in tuning the local immune response to establish equilibrium between disseminated nodal CSC and the immune system. *Cancer Res; 75(10); 2095–108. ©2015 AACR.*

Introduction

Metastatic disease is a dreadful complication of primary cancer, and the principal cause of cancer-related death. Two models explain the process of systemic cancer progression (1). The linear progression paradigm posits that tumor ontogeny occurs in the primary tumor, and only thereafter, disseminated tumor cells (DTC) deploy to sites of metastasis. Thus, the larger is the size of the primary tumor, the higher is the chance of metastatic spread. Conversely, the parallel progression model claims that tumor cells abandon the primary lesion before the acquisition of full malignant phenotype, and seed secondary growths where DTC undergo a stepwise progression of morphologic abnormalities. This model predicts greater genetic and epigenetic disparities between primary tumor cells and metastasis founders. Indeed, in several solid tumors, DTC exhibit significantly fewer genetic abnormalities than primary tumor cells, and heterogeneous chromosomal rearrangements can be found in primary tumors and DTC from different sites. The concept of early dissemination of tumor cells is also supported by the demonstration that in breast cancer models shortly after expression of the oncogenic transgene, neoplastic epithelial cells from atypical ductal hyperplasia disseminate to the lungs and bone marrow (2). Also, in women, bone marrow dissemination can occur at the stage of ductal carcinoma *in situ* (2).

Recent evidence strongly supports the role of cancer stem–like cells [CSC; (3)] in the metastatic process (4), and pancreatic epithelial cells with stem cell properties may invade the liver before frank malignancy is detected in the pancreas (5).

Once the DTC has reached the site of future metastasis, it has to survive and protect itself from immune surveillance (6). Indeed, *in vitro* CSC are killed by NK and T cells (7, 8), but also inhibit T-cell proliferation and effector function (9) through yet

[1]Division of Immunology, Transplantation and Infectious Diseases, Cellular Immunology Unit, IRCCS San Raffaele Scientific Institute, Milan, Italy. [2]Università Vita-Salute San Raffaele, Milan, Italy. [3]Division of Regenerative Medicine, Neural Stem Cell Unit, IRCCS San Raffaele Scientific Institute, Milan, Italy. [4]Crs4, Biomedicine Sector, Scientific Park of Sardinia, Pula, Cagliari, Italy. [5]Mass Spectrometry Unit, IRCCS San Raffaele Scientific Institute, Milan, Italy. [6]Unità Operativa Anatomia Patologica, IRCCS San Raffaele Scientific Institute, Milan, Italy.

Note: Supplementary data for this article are available at Cancer Research Online (http://cancerres.aacrjournals.org/).

Current address for E. Jachetti: Department of Experimental Oncology and Molecular Medicine, Molecular Immunology Unit, Fondazione IRCCS Istituto Nazionale dei Tumori, 20133 Milan, Italy; current address for S. Mazzoleni, Epigenetic Unit, Fondazione Istituto Nazionale Genetica Molecolare (INGM)—Ospedale Policlinico, 20122 Milan, Italy; current address for I.S. Piras, Unit of Child and Adolescent NeuroPsychiatry, Laboratory of Molecular Psychiatry and Neurogenetics, University "Campus Bio-Medico," 00128 Rome, Italy; and current address for U. Restuccia and A. Bachi, IFOM Istituto FIRC di Oncologia Molecolare, 20139 Milan, Italy.

R. Galli and M. Bellone contributed equally to this article.

Corresponding Author: Matteo Bellone, San Raffaele Scientific Institute, Via Olgettina 58, 20132 Milan, Italy. Phone: 39-0226434789; Fax: 39-0226434786; E-mail: bellone.matteo@hsr.it

doi: 10.1158/0008-5472.CAN-14-2346

undefined mechanisms. Nothing is known about CSC–T cell interactions *in vivo*.

The transgenic adenocarcinoma of the mouse prostate (TRAMP) model relies on the SV40 early genes (small and large T antigens; Tag) expressed under the control of the rat probasin regulatory element, so that Tag appears at puberty selectively on the prostate epithelium (10). TRAMP mice progressively develop mouse prostate intraepithelial neoplasia (mPIN; week 6–12), adenocarcinoma (week 12–18), and lymph node (LN) and lung metastases (week 18–30) resembling the human pathology (11). CSCs obtained from prostates of 10- to 11-week-old TRAMP mice affected by mPIN [hereafter named TPIN-SC; (12)] express prostate cancer–associated antigens, MHC I and MHC II molecules, and ligands for NK cells. Indeed, CSC can be targeted by NK and cytotoxic T lymphocytes (CTL) both *in vitro* and *in vivo* (13). Nonetheless, they generated tumors when injected in immunocompetent mice (13), suggesting they possess mechanisms of immune evasion. Concomitantly, at that age, TRAMP males develop full CTL tolerance to Tag (14), which behaves in this model as a tissue-restricted tumor-associated antigen. We then asked whether TPIN-SC adopt strategies to overcome immune surveillance. Here, we show that TPIN-SC precociously disseminated to prostate draining LN (PDLN), and used Tenascin-C (TNC), an extracellular matrix (ECM) disulfide-linked hexameric glycoprotein (15) to inhibit T-cell proliferation and effector function.

Materials and Methods

Mice, cell lines, and reagents

C57BL/6, C57BL/6-Tg(TcraTcrb)425Cbn/Crl, C57BL/6-Tg (TcraTcrb)1100Mjb/Crl (Charles River), and B6.129S7-Rag1tm1-Mom/J mice (16) were housed in a pathogen-free animal facility. The latter two were crossed to obtain RAG-$1^{-/-}$OT1 mice. Heterozygous TRAMP mice (10) were generated as described previously (14). Animals were treated in accordance with the European Community guidelines and with the approval of the Institutional Ethical Committee. Prostate CSC were cultured as described previously (12). Human peripheral blood mononuclear cells (PBMC) and B16-OVA melanoma cells (17) were cultured in IMDM (Lonza).

Cell cultures

Prostate CSCs were cultured in serum-free DMEM/F12 (Lonza) containing EGF and FGF2. Murine splenocytes were cultured in T-cell medium (TCM), composed by RPMI (Lonza), with 8% fetal bovine serum (FBS; Invitrogen), 2 mmol/L L-glutamine, 150 U/mL streptomycin, and 200 U/mL penicillin (Cambrex), 10 mmol/L Hepes, 10 mmol/L sodium pyruvate and 5 μmol/L β-mercaptoetanol (Gibco-Invitrogen). Human PBMC and B16-OVA melanoma cells were cultured in IMDM (Lonza), with 10% FBS (Invitrogen). Unless specified, all chemical reagents were from Sigma-Aldrich. Peptides were kindly provided by R. Longhi (CNR, Milan, Italy).

Proliferation assays

Splenocytes were labeled with CFSE, and activated *in vitro* with anti-CD3 and anti-CD28 beads (Invitrogen) and IL2 (R&D Systems) according to the manufacturer's instructions. When needed, irradiated (50 Gy) prostate CSCs were added in coculture or in a Transwell system (0.4 μm) at the indicated CSC: splenocyte ratio. When indicated, soluble TNC (0.5μg/mL; R&D Systems) was added, or splenocytes were incubated with 0.5 μg/mL of isoDGR (18) and/or beads coated with anti-α_5 (CD49e) antibody (clone 5H10-27; 66μg/mL; BioLegend) 30 minutes before the addition of prostate CSC. CFSE-labeled splenocytes from transgenic OTII or Rag-$1^{-/-}$ OTI mice were cocultured with irradiated CSC in the presence of $OVA_{323-339}$ (20 ng/mL) or $OVA_{257-264}$ (10 ng/mL) peptides, respectively, and 3.5 ng/mL of IL12 (R&D Systems). After 3 or 5 days, respectively, cells were analyzed by FACS. PDLN from TRAMP or wild-type (WT) mice were digested with collagenase IV (1,600 U/mL) for 1 hour at 37°C, labeled with CFSE, activated as described above, and analyzed after 3 days by FACS. When indicated, mice were treated i.p. (5 d/wk) with either AMD3100 (3.5 mg/kg) or vehicle from week 4 to 12 of age. Human PBMC isolated from buffycoats of healthy subjects, who gave their informed consent, were labeled with CFSE, activated with concanavalin A (5 μg/mL), and cultured and analyzed as described above.

In vivo proliferation

Procedures are reported in Supplementary Materials and Methods.

Stable isotope labeling with amino acids in cell culture, mass spectrometry, and data analysis

OTI cells were activated as described above and cultured in SILAC (stable isotope labeling with amino acids in cell culture) medium containing light (^{12}C and ^{14}N) or heavy (^{13}C ^{15}N) labeled L-lysine and L-arginine, in the presence of irradiated prostate CSC. After 7 days of coculture, $CD8^+$ T cells from either condition were sorted for activated ($CD8^+CD62L^{low}$) or inhibited ($CD8^+CD62L^{high}$) phenotype and lysed in RIPA buffer (Cell Signaling Technology). Heavy and light lysates were mixed at 1:1 for protein content; proteins were then resolved onto a 4% to 12% NuPAGE precast gel (Invitrogen) and stained by Coomassie colloidal blue. The gel lane was cut into 12 slices, each of which was reduced, alkylated, and digested with trypsin as reported previously (19). Mass spectrometry (MS) procedures, according to ref. 20, and analysis of differentially expressed proteins in T cells from SILAC cultures are described in Supplementary Material and Methods.

Microarray-based gene expression profiling

Procedures are reported in Supplementary Materials and Methods.

Silencing of TNC

TPIN-SC were stably infected with TNC shRNA Lentiviral Particles or with control shRNA Lentiviral Particles (Santa Cruz Biotechnology, Inc.) as described in Supplementary Materials and Methods.

Flow cytometry, immnohistochemistry, immunofluorescence, and Western blot analysis

Procedures are described in Supplementary Material and Methods.

Generation of CSC from LN

PDLN, or axillary LN as control, were isolated and digested with collagenase IV (1,600 U/mL) for 1 hour at 37°C. Cells were seeded in a serum-free medium containing EGF and

FGF2, and cultures were splitted every 2 to 10 days, according to the stage of origin (12).

Real-time PCR

Real-time PCR was performed and analyzed using the $\Delta\Delta C_T$ method as described in Supplementary Experimental Procedures.

Statistical analyses

Statistical analyses were performed using the Student *t* or one-way ANOVA followed by Tukey tests. Values were considered statically significant for *, $P < 0.05$; **, $P < 0.01$; ***, $P < 0.001$.

Results

CSC from autochthonous mPIN lesions dampen T-cell activation

To investigate potential interactions between CSC and the immune system in the early phases of neoplastic transformation, we took advantage of TPIN-SC, which were obtained from young TRAMP mice affected by mPIN, and TNE-SC isolated from neuroendocrine lesions developed in 30-week-old TRAMP mice (12). Both CSC types fulfilled the criteria of endless self-renewal ability, multi-lineage differentiation, and tumorigenic potential (12). However, gene expression analysis revealed that the two CSC types were remarkably different, resembling the stages of progression of human prostate cancer (12).

CFSE-labeled naïve splenocytes were cultured with anti-CD3/CD28 beads alone or in the presence of irradiated TPIN-SC or TNE-SC. Flow cytometry analysis of $CD4^+$ and $CD8^+$ T cells showed that in the presence of TPIN-SC, most of the T cells underwent growth arrest soon after activation (Fig. 1A). This phenomenon was highest at the CSC:splenocyte ratio 1:10 (Fig. 1B), and required cell-to-cell contact (Fig. 1A). Interestingly, TNE-SC did not inhibit T-cell proliferation (Fig. 1A), thus demonstrating that dampening T-cell activation is a peculiar characteristic of TPIN-SC.

Both $CD4^+$ and $CD8^+$ T cells in the presence of TPIN-SC and CD3/CD28 beads received an activation signal strong enough to induce upregulation of several activation markers, including CD44 and LFA-1 (Fig. 1C and Supplementary Fig. S1A). However, in those cells, CD69 remained exceedingly upregulated, whereas CD25 did not reach the expression levels of fully activated T cells (Fig. 1D and Supplementary Fig. S1B). Aborted activation was confirmed by the lack of CD62L downregulation, (Fig. 1D and Supplementary Fig. S1B). Moreover, T cells cultured with TPIN-SC showed a higher expression of CCR6 and a lower expression of CXCR3, the latter being a characteristic of very recently activated T cells, while, as expected, it was upregulated in fully activated T cells (Fig. 1E and Supplementary Fig. S1C). In line with the observation that CXCR3 is required for optimal IFNγ production by T cells (21), the frequency of $IFN\gamma^+$ T cells was dramatically reduced in TPIN-SC-splenocyte cocultures (Fig. 1E and Supplementary Fig. S1C), confirming that TPIN-SC interfered with full activation of T cells. TPIN-SC–mediated T-cell inhibition was not species specific, because also proliferation of human PBMCs was inhibited by TPIN-SC and not by TNE-SC (Fig. 1F and Supplementary Fig. S1D).

To verify that T-cell inhibition ability was a peculiarity of TPIN-SC and not an artifact of irradiation, which can induce release of inhibitory molecules, we repeated the above-described experiments with nonirradiated CSC. In line with the results reported in Fig. 1, nonirradiated TPIN-SC inhibited proliferation (Supplementary Fig. S2A) and IFNγ production (Supplementary Fig. S2B and S2C) of both $CD4^+$ and $CD8^+$ T cells in a cell-to-cell contact fashion (Supplementary Fig. S2A). As expected, nonirradiated TNE-SC had no effect on T-cell proliferation and cytokine production (Supplementary Fig. S2).

Also, antigen-specific proliferation and IFNγ production induced by ovalbumin (OVA) in both OTII and OTI transgenic T cells, which express TCR specific for OVA (22, 23), were inhibited by TPIN-SC (Fig. 2A) and not by TNE-SC (data not shown). Of relevance, coculture with TPIN-SC did not increase the number of Annexin V^+ T cells, ruling out the possibility that CSC favor T-cell apoptosis (Fig. 2B).

To verify whether inhibition occurs also *in vivo*, a mixture (10:1 ratio) of naïve CFSE-labeled OTI cells and irradiated TPIN-SC was injected in the spleen of C57BL/6J mice bearing a well-established B16-OVA melanoma (17). Their spleens and tumors were collected 5 days later, to quantify infiltrating $CFSE^+$ cells. The presence of TPIN-SC associated with a reduced expansion of OTI cells in the spleen, and a reduced tumor infiltration by OTI cells, thus confirming the immunosuppressive activity of TPIN-SC also *in vivo* (Fig. 2C).

TPIN-SCs also inhibited restimulation of previously activated T cells. When splenocytes were collected from mice that had been vaccinated with dendritic cells pulsed with Tag (14), and restimulated *in vitro*, coculture with TPIN-SC dampened proliferation and IFNγ production (Supplementary Fig. S3A) and cytolytic activity (Supplementary Fig. S3B), whereas TNE-SC were ineffective. As for naïve T cells, inhibition of antigen-experienced T cells required cell-to-cell contact (Supplementary Fig. S3A and S3B). Notably, when TPIN-SC were added to the culture of fully activated $CD4^+$ and $CD8^+$ T cells, no inhibitions in subsequent T-cell proliferation and cytokine production were measured (Supplementary Fig. S3C).

Collectively, these data suggested that TPIN-SC acted during the early steps of T-cell activation. Phosphorylation of ZAP70, ERK2, and STAT5, all proximal signaling events linked to TCR and IL2 receptor triggering, respectively, was significantly reduced in T cells activated in the presence of TPIN-SC (Supplementary Fig. S4A). Thus, TPIN-SC–conditioned T cells might have acquired phenotypic and functional characteristics of hypo-responsive lymphocytes (24). To assess this possibility, SILAC and MS procedures were implemented to quantify protein variations in cocultures of T cells with CSCs. Proteins extracted from T cells inhibited by the presence of TPIN-SCs (sorted for being $CD62L^{hi}$) and from fully activated T cells in the presence of TNE-SCs (sorted for being $CD62L^{low}$; Supplementary Fig. S4B) were analyzed by high-resolution MS, allowing the reliable identification and quantification of about 1,000 proteins (Supplementary Fig. S4B). Statistical analysis by MaxQuant highlighted 100 of them to be differentially expressed ($P < 0.05$; Supplementary Table S1) and query of Gene Ontology and KEGG databases showed that proteins involved in cytoskeleton organization and glucose metabolism were significantly modified in T cells after coculture with TPIN-SCs (Supplementary Table S2). Interestingly, TPIN-SC–conditioned T cells maintained upregulated proteins involved in

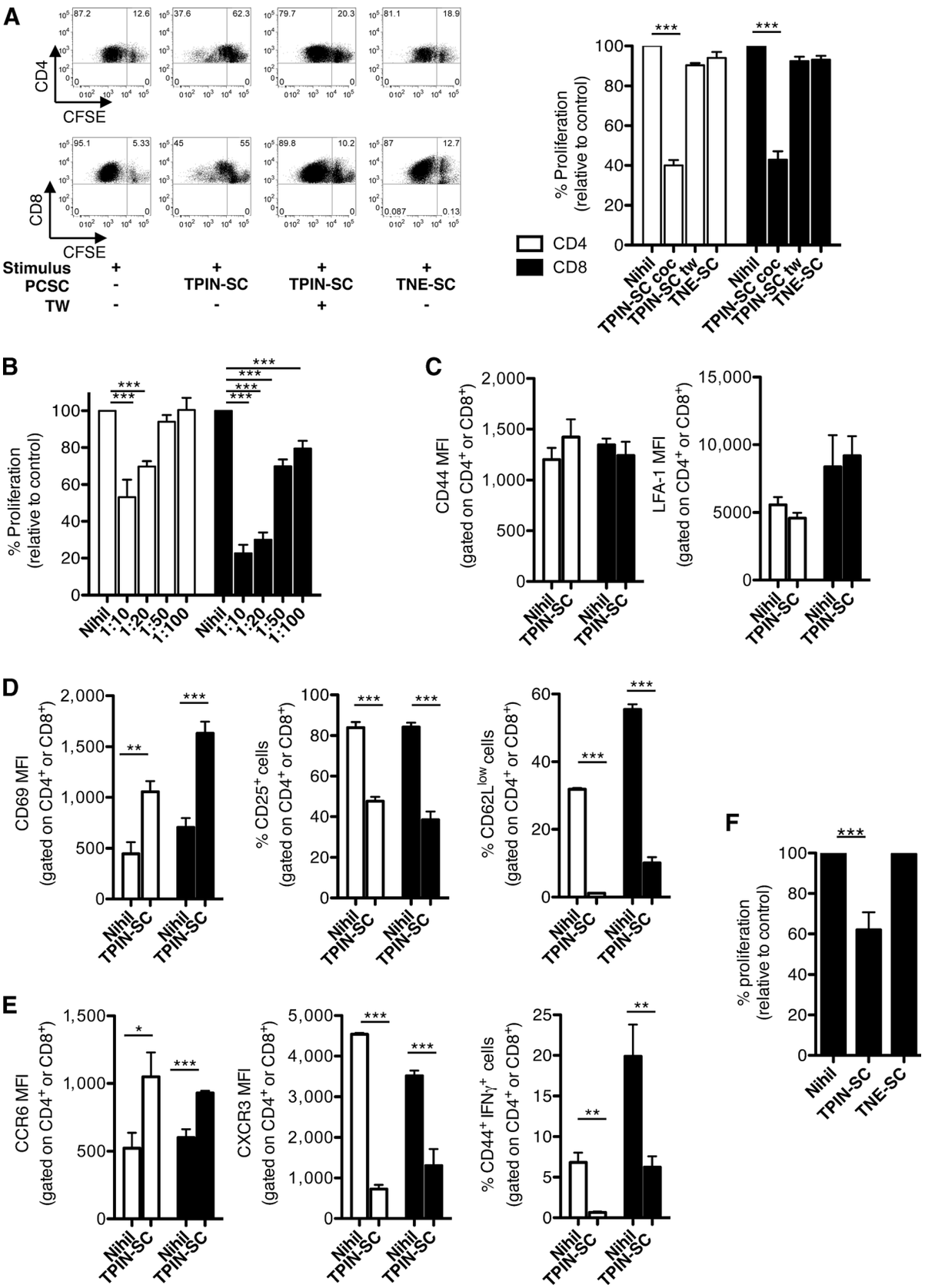

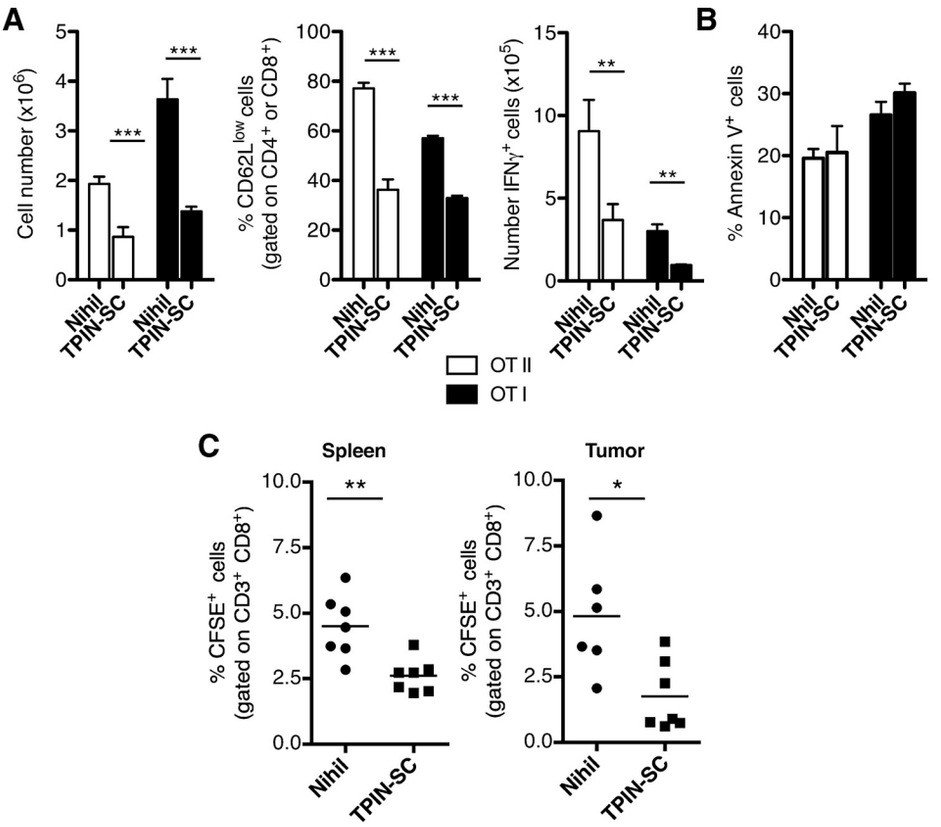

Figure 2.
TPIN-SC dampen antigen-specific T-cell activation both *in vitro* and *in vivo*. A and B, OTII ($CD4^+$; white bars) and OTI ($CD8^+$; black bars) cells were primed *in vitro* with $OVA_{323–339}$ and $OVA_{257–264}$ peptides, respectively, alone (Nihil) or in the presence of irradiated TPIN-SCs (ratio, 1:10), and analyzed after 3 (OTI) or 5 (OTII) days for proliferation (left), expression of activation markers (middle), IFNγ production (right; A), or apoptosis (B). C, C57BL6J mice bearing s.c. B16-OVA melanoma (at least 4 × 4 mean diameter) were inoculated intra-spleen with 30×10^6 CFSE-labeled splenocytes from RAG-$1^{-/-}$ OTI mice, together or not with 3×10^6 TPIN-SCs. After 5 additional days, mice were killed, and $CFSE^+CD3^+CD8^+$ cells in the spleens and tumors were quantified by FACS. Data are representative of at least three independent experiments. Data are reported as average ± SD. The Student *t* test: *, $P < 0.05$; **, $P < 0.01$; ***, $P < 0.0001$.

pyruvate metabolism (Supplementary Table S2), which is a peculiarity of resting T cells (25), and failed to upregulate the amino acid transporter CD98 and the transferrin receptor CD71 (Supplementary Fig. S4B), suggesting an impaired change of the metabolic machinery, a characteristic of anergic T cells (25). When $CD8^+$ T cells were sorted from cultures of either T cells alone or with TPIN-SCs, and subjected to a second round of stimulation in the absence of TPIN-SCs, they proliferated and downregulated CD62L in comparable way (Supplementary Fig. S4C), demonstrating that the TPIN-SC–mediated T-cell hyporesponsiveness is reversible.

TNC is overexpressed in TPIN-SC and in both human and TRAMP prostate cancer lesions and is involved in TPIN-SC–mediated immunosuppression

We compared the transcriptome of TPIN-SC with that of TNE-SC (12), founding 37 differentially expressed genes (fold change > 2; $P < 0.001$), among which we identified the ECM protein TNC, upregulated in TPIN-SC (Fig. 3A) as a potential immunosuppressive molecule. TNC provides physical and signaling support for CSC and metastasis initiating cells (26), and can be immunosuppressive *in vitro* (27), yet each of these functions had been independently reported.

Expression of TNC in TPIN-SC and not in TNE-SC was confirmed by both Western blot analysis (Fig. 3B), and immunofluorescence (Fig. 3C). Moreover, when soluble TNC, whose sequence is conserved between humans and mice, was added to the cultures of human (Fig. 3D) or mouse T cells (Fig. 3E), it mirrored the effects of TPIN-SC on proliferation, expression of CD62L, and cytokine production. Thus, TNC was a strong candidate for mechanistic TPIN-SC–mediated immunosuppression.

Whereas in the prostate of WT mice at any age (Fig. 4A), expression of TNC was absent (Fig. 4B); in mPIN lesions from

Figure 1.
TPIN-SC arrest *in vitro* T-cell activation. A, left, representative dot plots of *in vitro* proliferation of $CD4^+$ (top) and $CD8^+$ splenocytes (bottom) measured by FACS as CFSE dilution after 5 or 3 days, respectively, of stimulation with anti-CD3/CD28 beads alone (Nihil) or in the presence of irradiated TPIN-SC or TNE-SC. CSCs (1:10 ratio) were added in coculture (coc) or in the upper chamber of a 0.4-mm Transwell (tw). Right, percentage of proliferating $CD8^+$ (black bars) and $CD4^+$ (white bars) T cells. B, titration of TPIN-SC–mediated inhibition of $CD8^+$ (black bars) and $CD4^+$ (white bars) T-cell proliferation at the indicated CSC:splenocyte ratio. D–E, expression (MFI, mean fluorescence intensity) of cell-surface markers and percentage of cells producing IFNγ in cultured $CD8^+$ (black bars) and $CD4^+$ (white bars) T cells. F, proliferation of PBMC as measured by CFSE dilution at day 6 of stimulation with ConA alone (Nihil) or in the presence of irradiated TPIN-SC or TNE-SC (1:10 ratio). Each panel of the figure is representative of at least three independent experiments. Data are reported as average ± SD. ANOVA followed by the Tukey test and the Student *t* test: *, $P < 0.05$; **, $P < 0.01$; ***, $P < 0.0001$.

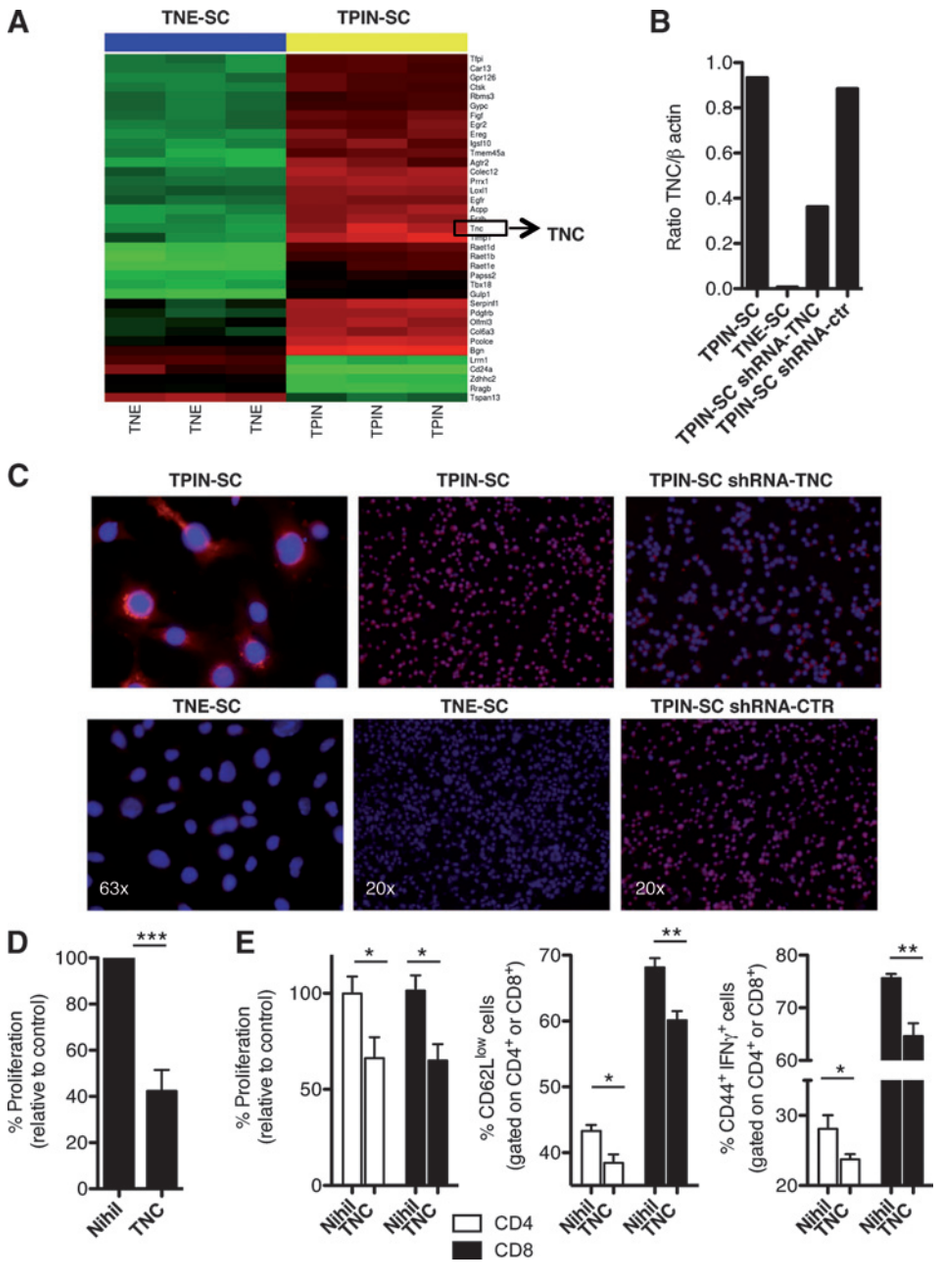

Figure 3.
TNC is expressed in TPIN-SC and inhibits T-cell priming. A, gene expression analysis of CSC with Affimetrix Mouse Gene 1.0 ST Array. Heatmap reports the global gene expression data in TPIN-SCs versus TNE-SCs. Differentially expressed genes with a $P < 0.001$ are red (upregulated) or green-colored (downregulated). B, Western blot analysis for TNC expression in CSC reported in A. C, immunofluorescence analysis for TNC expression in TPIN-SC, TNE-SC, or TPIN-SC infected with lentiviral vectors encoding for anti-TNC (TPIN-SC shRNA-TNC) or unspecific (TPIN-SC shRNA-ctr) shRNA (red, TNC; blue, DAPI;). D, proliferation (i.e., CFSE dilution measured at FACS) of PBMC at day 6 of stimulation with ConA alone (Nihil) or in the presence of soluble TNC (0.5 μg/mL). E, CFSE dilution (left), expression of CD62L (middle), and IFNγ production (right), as measured by flow cytometry, in $CD4^+$ (white columns) and $CD8^+$ splenocytes (black columns) at days 5 or 3, respectively, of stimulation with anti-CD3 and anti-CD28 beads alone (Nihil) or in the presence of TNC (0.5 μg/mL). Data are representative of at least three independent experiments. Data are reported as average ± SD. The Student *t* test: *, $P < 0.05$; **, $P < 0.01$; ***, $P < 0.0001$.

TRAMP mice (Fig. 4A), TNC showed a patchy distribution mostly within the stroma surrounding affected acini, and in a few transformed epithelial cells (Fig. 4B). A faint cytoplasmic expression of TNC was present in TRAMP adenocarcinoma cells (Fig. 4B), and absent in neuroendocrine tumors (Fig. 4B). In good correlation with the TRAMP model, TNC was expressed in human PIN (Fig. 4B), and not in human adenocarcinoma (Fig. 4B). TNC was also expressed in metastatic LN, confirmed by cytokeratin staining (Fig. 4C), of both TRAMP (Fig. 4C) and prostate cancer patients (Fig. 4C), but not in metastatic LN from TRAMP mice affected by neuroendocrine tumors (Fig. 4C, middle).

TPIN-SC were infected with lentiviral vectors encoding either a TNC-specific or a scrambled short hairpin RNA (shRNA-TNC and shRNA-ctr, respectively). Both Western blot analysis (Fig. 3B) and immunofluorescence (Fig. 3C) confirmed the specific silencing of TNC. Reduction of TNC expression in TPIN-SC did not influence their *in vitro* growth, because TPIN-SC infected with either shRNA-TNC or shRNA-ctr showed similar growth rate (data not shown). However, specific silencing of TNC substantially dampened the effects of TPIN-SC on T-cell proliferation and modulation of activation markers (Fig. 5A), and fully rescued the capacity of T cells to produce IFNγ upon activation (Fig. 5A). This was confirmed by the increase of ZAP70 and ERK2 phosphorylation levels (Fig. 5B and Supplementary Fig. S5A and S5B). Thus, TNC is directly involved in TPIN-SC–mediated immunosuppression. Interestingly, silencing of TNC did not abrogate the inhibition

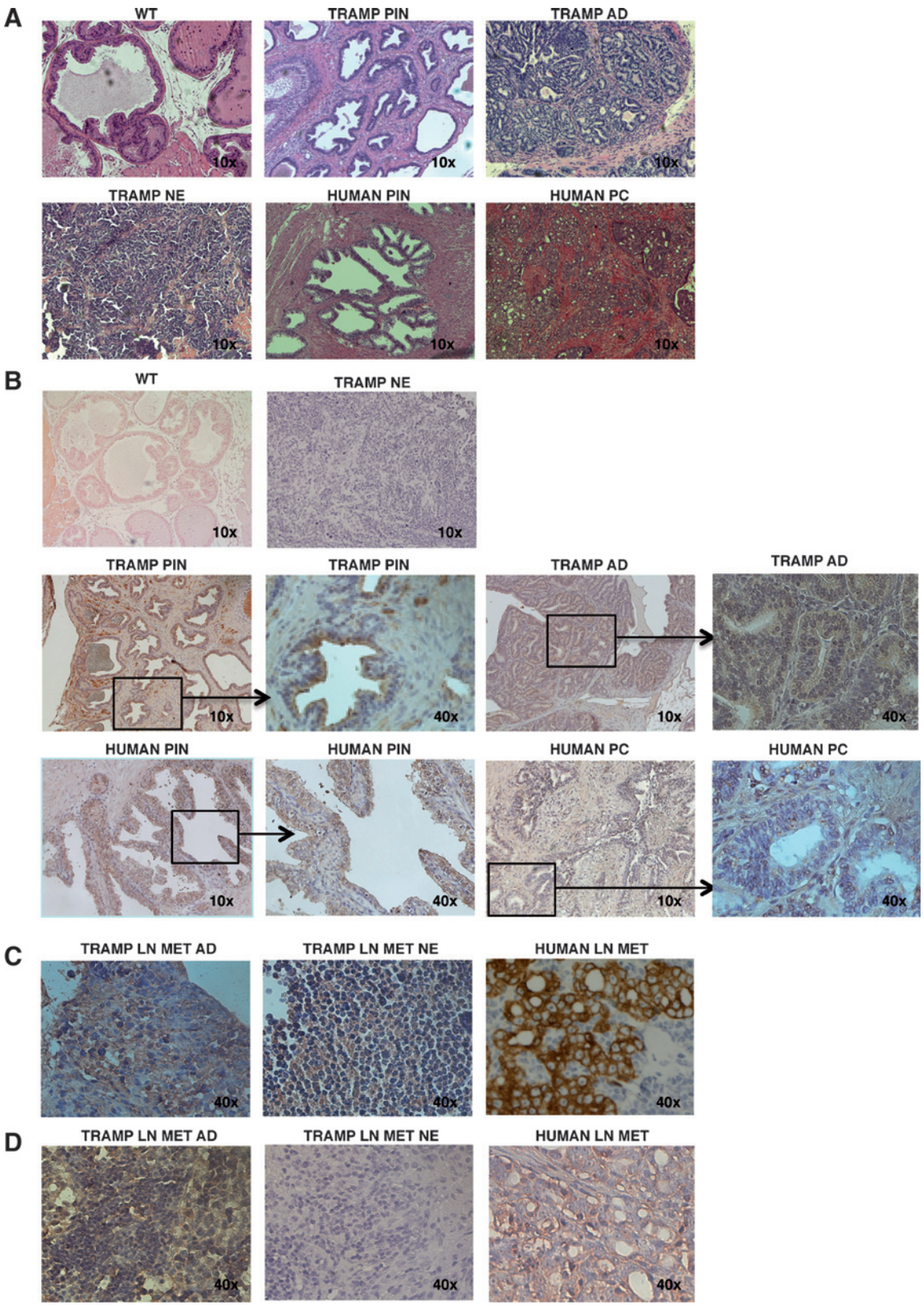

Figure 4.
TNC expression in mouse and human prostates and metastatic LN. A–D, hematoxylin and eosin staining (A), immunohistochemistry for TNC (B and D), or pan-cytokeratin (C) on the indicated samples. Slides are representative of at least three different cases.

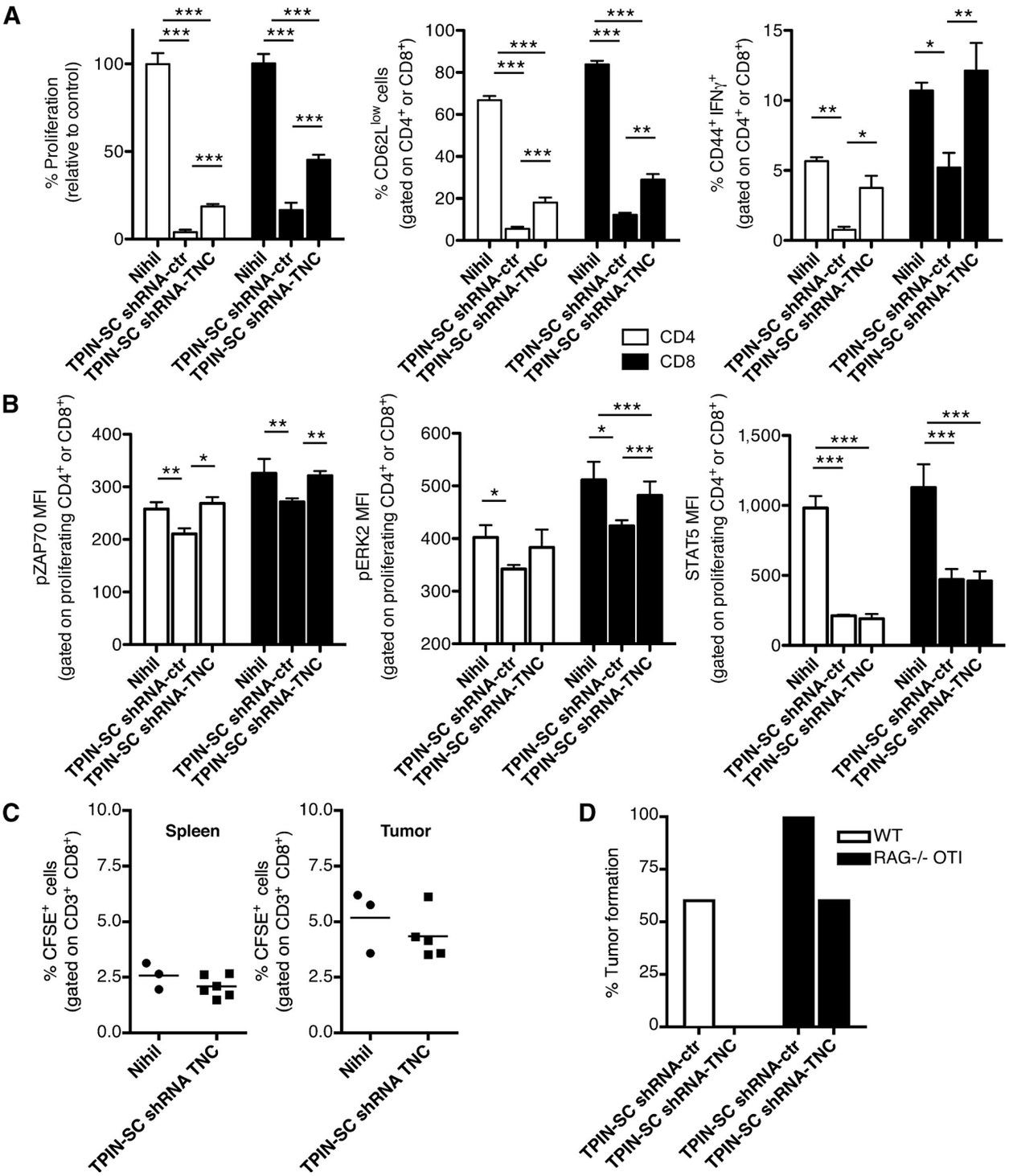

Figure 5.

Silencing of TNC modulates the inhibitory activity of TPIN-SC. A, CFSE dilution (left), expression of CD62L (middle), or IFNγ production (right) by $CD4^+$ (white columns) and $CD8^+$ splenocytes (black columns) at days 5 or 3, respectively, of stimulation with anti-CD3/CD28 beads alone (Nihil) or in the presence of irradiated TPIN-SC shRNA-TNC or TPIN-SC shRNA-ctr (1:10 ratio). B, phosphorylation of Zap70 (pZAP70), ERK (pERK), and STAT5 (pSTAT5) in cells described in A as measured by FACS. C, FACS analysis of spleen and tumor cells from B16-OVA–bearing mice treated as described in Fig. 3C, with the exception that CFSE-labeled splenocytes were inoculated together or not with 3×10^6 TPIN-SC shRNA-TNC. D, frequency of tumor formation in C56BL/6 (WT; white bars) or RAG-$1^{-/-}$ OT1 male mice (OT1; black bars; $n = 5$ for each group) challenged s.c with 2×10^6 TPIN-SC shRNA-TNC or TPIN-SC shRNA-ctr mixed 1:1 with Matrigel. Mice with no apparent tumor were sacrificed 100 days after challenge. Each panel of the figure is representative of at least two independent experiments performed with at least 3 mice per group. Data are reported as average ± SD. ANOVA followed by the Tukey test and Student *t* test: *, $P < 0.05$; **, $P < 0.01$; ***, $P < 0.0001$.

of TPIN-SC of STAT5 phosphorylation (Fig. 5B and Supplementary Fig. S5C), suggesting that TNC does not affect IL2 signaling pathway, and that additional mechanisms cooperate in the immunosuppressive activity of TPIN-SC on T cells.

TNC silencing abrogated the inhibitory activity of TPIN-SC on T cells also *in vivo*. Indeed, the frequency of CFSE-labeled OTI cells was similar in the spleens and tumors of mice bearing B16-OVA melanoma, irrespective of the fact that they were infused 5 days earlier with naïve CFSE-labeled OTI cells either admixed or not to TPIN-SC-shRNA-TNC cells (Fig. 5C).

TPIN-SC infected with either shRNA-TNC or shRNA-ctr were injected subcutaneously within Matrigel plugs into fully immunocompetent C57BL/6 mice or RAG-$1^{-/-}$OT1 mice, which lack B and T cells but OVA-specific $CD8^+$ T cells. In agreement with our previous findings (13), TPIN-SC-shRNA-ctr cells generated tumors in 100% of RAG-$1^{-/-}$OT1 mice, and 60% of C57BL/6 mice (Fig. 5D), supporting a role for adaptive immunity in surveillance against TPIN-SC–derived tumors. Because no tumor grew in C57BL/6 mice challenged with TPIN-SC-shRNA-TNC cells (Fig. 5D), we conclude that TNC produced by TPIN-SCs negatively affected adaptive immune surveillance. TNC also has a function on tumor biology, because only 60% of RAG-$1^{-/-}$OT1 mice developed tumor upon challenge with TPIN-SC-shRNA-TNC cells (Fig. 5D).

TNC produced by CSC interacts with α5β1 integrin and inhibits T-cell proliferation by blocking stress fiber formation

TPIN-SC required a cell-to-cell contact to arrest T-cell activation (Fig. 1A). To further investigate the role of TNC in this cell-to-cell interaction, contacts between CFSE-labeled prostate CSC and CMTMR-labeled CD8 T cells were recorded by multichannel time-lapse fluorescent live cell imaging during the first 4 hours of coculture (Fig. 6A). Stimulated T cells were engaged in more prolonged contacts with TPIN-SC than with TNE-SC, and, more importantly, silencing of TNC in TPIN-SC reduced

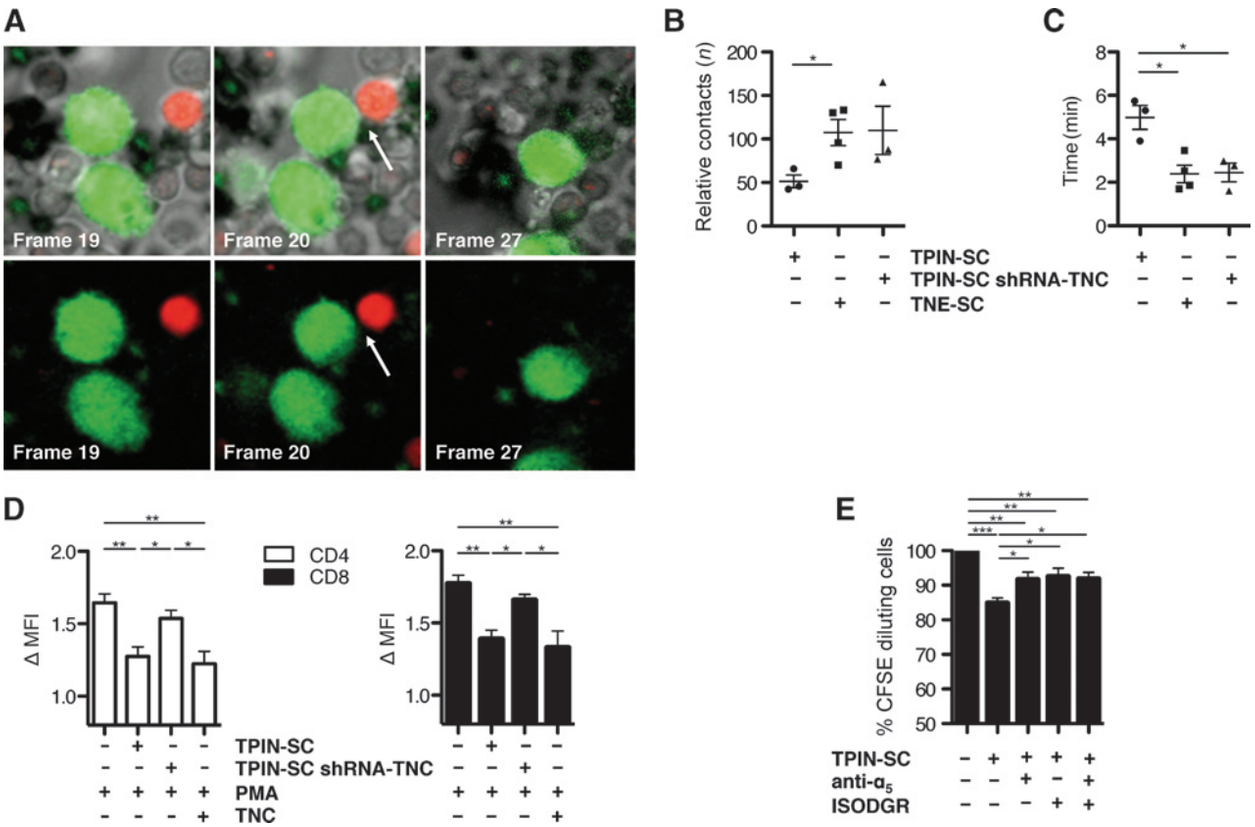

Figure 6.

TNC inhibits lymphocyte actin polymerization and proliferation through integrin α5β1. A, CFSE-labeled TPIN-SC, TNE-SC, or TPIN-SC shRNA-TNC were cultured with CMTMR-labeled $CD8^+$ T cells (ratio, 1:10) in the presence of anti-CD3/CD28 beads. The images refer to representative frames from a 10-frame sequence (ΔT = 3 minutes) of the coculture of TPIN-SC with $CD8^+$ T cells. Top, merge of bright and fluorescent channels; bottom, fluorescent channels. B, quantification of number (*n*) of relative cell contacts calculated after normalization for total cell counts. C, quantification of the average contact time (in minutes) calculated by dividing the movie duration by the total number of contacts. D, splenocytes were treated with CCD (data not shown) or cocultured with TPIN-SC, TPIN-SC, shRNA-TNC (ratio, 10:1) or in the presence of TNC (0.5 μg/mL), followed by PMA stimulation. F-actin polymerization of $CD4^+$ (white bars) and $CD8^+$ (black bars) T cells is represented as the ratio of the mean fluorescence intensity (MFI) values after and before PMA stimulation. E, percentage of proliferating $CD8^+$ T cells stimulated for 3 days with anti-CD3/CD28 beads alone (Nihil) or cocultured with irradiated TPIN-SCs (right) or with TPIN-SCs shRNA-TNC (left) ± isoDGR and/or beads coated with anti-α5 antibodies. Each panel of the figure is representative of at least three independent experiments. E, aggregated data from three independent experiments. Data are reported as average ± SD. ANOVA followed by the Tukey test and the Student *t* test: *, $P < 0.05$; **, $P < 0.01$; ***, $P < 0.0001$.

the duration of contacts to the level of TNE-SC (Fig. 6B and C). Thus, TNC appeared to be directly involved in CSC–T cell contacts, eventually leading of T-cell inhibition.

Intracellular signaling triggered by TCR stimulation is intimately related to the reorganization of the actin/myosin and microtubule cytoskeleton through small GTPases, including Rho, Rac, and Cdc42 (28). Inhibition of Rho in T cells suppresses T-cell proliferation (29), and TNC inhibits Rho activation (30). Thus, we hypothesized that TNC arrests T-cell proliferation by inhibiting cytoskeleton reorganization. In support of this hypothesis, SILAC analysis on T cells inhibited by TPIN-SC showed downregulation of actin gamma 1 (Actg1) and myosin heavy chain 10 (Myh10), two molecules involved in actin stress fibers assembly and focal adhesion formation (Supplementary Table S1). SILAC analysis revealed that other molecules involved in Rho and Rac pathways were differentially expressed in T cells inhibited by TPIN-SCs. Indeed, in TPIN-SCs conditioned T cells, we found upregulation of the Rho GDP dissociation inhibitors 1 and 2 (Arhgdia and Arhgdib), which prevent Rho activation by blocking the release of GDP, an essential step for GTP loading and activation (Supplementary Table S1; ref. 31). Cofilin, a downstream effector of both RhoA and Rac, which inhibits actin polymerization (32) was also upregulated in TPIN-SC–conditioned T cells (Supplementary Table S1). Conversely, the Rho GTPase-activating protein 1 (Arhgap1) was downregulated (Supplementary Table S1). Also Crk, which can activate small GTPAses including Rac (33), and the Rac downstream effectors Vinculin and Gelsolin were downregulated in TPIN-SCs conditioned T cells (Supplementary Table S1).

Thus, to corroborate the hypothesis that TNC inhibits cytoskeleton reorganization, polymers of F-actin were quantitated in T cells by staining with FITC-conjugated phalloidin. As expected, T cells increased actin polymerization after PMA stimulation and this process was inhibited by pretreatment with cytocalasin D (Fig. 6D and data not shown), which selectively blocks the ATP-dependent actin polymerization process. Actin polymerization was inhibited also when T cells were activated in the presence of TPIN-SC or TNC and, most importantly, silencing of TNC in TPIN-SC rescued actin polymerization in both $CD4^+$ and $CD8^+$ T cells (Fig. 6D).

Several molecules can bind to TNC, including integrins (e.g., $\alpha2\beta1$, $\alpha5\beta1$), annexin II, and EGFR (15). To assess the role of integrins in the TNC-mediated inhibition of T-cell functions, the peptide isoDGR, which selectively inhibits interaction between $\alpha5\beta1$, $\alpha v\beta6$, and $\alpha v\beta8$ integrins and their ligands (18), or a blocking anti-$\alpha5$ monoclonal antibody (34) were added to TPIN-SC-T cells cultures. Because both reagents inhibited the suppressive activity of TPIN-SC, and the combination of the two reagents did result in neither additive nor synergy effects (Fig. 6E), we conclude that TNC mostly interacts with $\alpha5\beta1$ to deliver its immunosuppressive effect. Collectively, these findings demonstrate that TNC produced by CSC arrest T-cell activation by interacting with $\alpha5\beta1$ and blocking reorganization of actin-based cytoskeleton.

CSCs migrate to PDLN at the stage of mPIN and favor an immunosuppressive environment

Priming of naïve T cells and restimulation of memory T cells occur mostly in secondary lymphoid organs. Because TPIN-SC inhibited T-cell priming and restimulation, and in TRAMP mice, peripheral tolerance to Tag is reached at the stage of mPIN (14), we hypothesized that in TRAMP mice, CSC deploy early to PDLN, where they suppress T-cell activation. Indeed, TPIN-SC expressed CXCR4 (Supplementary Fig. S6A), which is essential for CSC-mediated tumor metastasis (4), and migrated *in vitro* through CXCL12. Moreover, the CXCR4 inhibitors AMD3100 and Peptide R (35) restrained their migration (Supplementary Fig. S6B and S6C). We found clear evidence that expression of CXCL12 was higher in PDLN from TRAMP mice, starting from week 8, than in NDLN of TRAMP mice or in PDLN of WT mice (Supplementary Fig. S6D). Interestingly, TPIN-SC did not express CCR7, and expressed low levels of CCR6 and CXCR3 (Supplementary Fig. S6E). Thus, CSC from mPIN lesions might primarily use the CXCR4–CXCL12 axis to migrate and deploy to PDLN.

Hence, we looked *ex vivo* for the presence of putative prostate CSC [enriched within the population of $CD45^-CD31^-CD44^+CD166^+Sca1^+$ cells; (13, 36)] in PDLN of TRAMP mice either young enough not to show any prostate lesion (6-week-old), or affected by full-blown tumor (16-week-old). PDLN from both 6-week-old TRAMP and WT mice did not contain any of these cells (Fig. 7A); conversely, they were enriched in PDLN of 16-week-old TRAMP mice. To investigate whether prostate CSC can disseminate from early primary lesions, PDLN and LN not draining the prostate (NDLN) from 12-week-old TRAMP affected by mPIN and WT mice were processed to single-cell suspension and cultured to generate CSC lines (12). Although PDLN from TRAMP mice gave rise to CSC lines (TLN-SC) with efficiency close to 80%, neither TRAMP NDLN nor PDLN and NDLN from WT mice ever gave rise to prostaspheres (Fig. 7B). TLN-SC showed a phenotype comparable with TPIN-SC, and substantially different from *ex vivo* whole prostate epithelial cells collected from age-matched TRAMP mice (Fig 7C). As confirmation of their origin, TLN-SC expressed the prostate antigens STEAP (37) and PSCA (Fig. 7D; ref. 38). We found higher TNC in TRAMP PDLN than in NDLN or PDLN of age-matched WT mice (Fig. 7E). More importantly, TLN-SC expressed TNC (Fig. 7F) and recapitulated the immunosuppressive effects of TPIN-SC on mouse T cells (Fig. 7G).

The existence of an immunosuppressive environment in PDLN of 12-week-old TRAMP mice was confirmed by the finding that $CD8^+$ T cells from TRAMP PDLN proliferated less than T cells from PDLN of age-matched WT mice (Fig. 7H). Importantly, when TRAMP mice were treated with AMD3100 starting at 4 weeks of age, $CD8^+$ T-cell proliferation in their PDLN at 12 weeks returned comparable with WT mice either treated or not with the drug (Fig. 7H).

Thus, CSCs early disseminate to PDLN, where they use TNC to avoid immune surveillance, and a precocious treatment with a CXCR4 inhibitor can positively affect local CSC-mediated immunosuppression.

Discussion

We have found that CSC, already at the stage of mPIN, deploy to PDLN that at pathologic examination appear as nonmetastatic. Thus, prostate cancer appears to adhere to the model of parallel metastatic spread (1). In support of this model, 13.3% of patients with pT3 prostate carcinoma treated by radical prostatectomy and bilateral LN dissection, and classified as node negative, harbored instead occult LN metastases, which were an independent predictor of recurrence and death in a multivariable analysis (39).

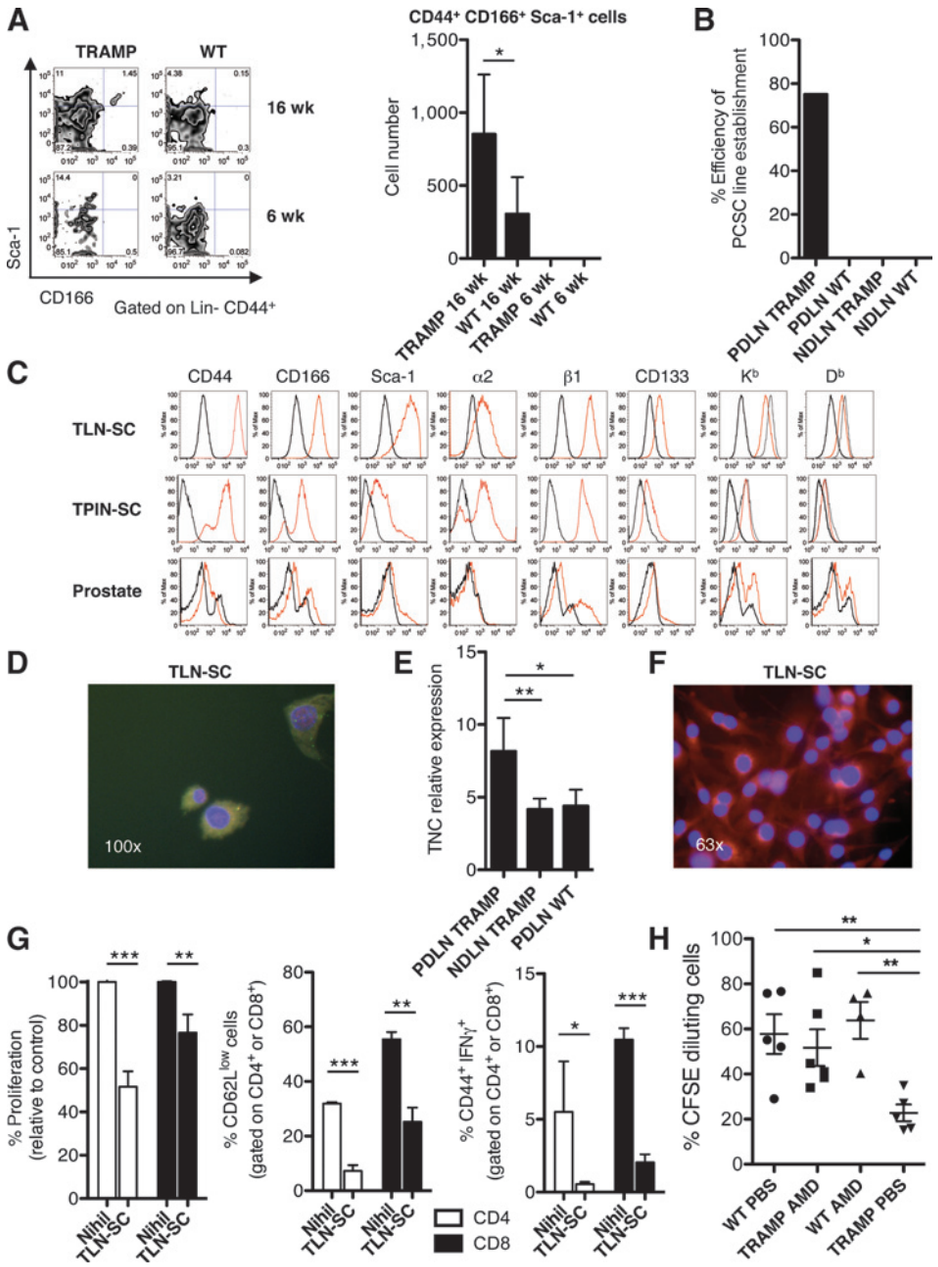

Figure 7.
PAC-SCs expressing TNC are present in PDLN. A, representative dot plots (left) and quantification (n≥5/group; right) of Lin$^-$(CD45$^-$CD31$^-$) CD44$^+$ Sca-1$^+$CD166$^+$ cells in PDLN from 16- or 6-week-old TRAMP and WT mice. B, percentage of success in establishing CSC lines from PDLN or NDLNs from 12-week-old TRAMP ($n = 4$/group) and WT mice ($n = 2$). C, FACS analysis of TLN-SC, TPIN-SC, or *ex vivo* prostate cells from 12-week-old TRAMP mice (red, specific staining; black, isotype control; gray, specific staining after IFNγ stimulation). D, STEAP (red) and PSCA (green) immunofluorescence on TLN-SCs (blue, DAPI). E, relative expression ± SD of TNC in PDLN or NDLN of TRAMP and WT mice as assessed by real-time PCR. Values were normalized to the positive control (i.e., TRAMP prostate). F, TNC immunofluorescence in TLN-SC (red, TNC; blue, DAPI). G, proliferation, expression of CD62L, and cytokine production (average ± SD) of CD4$^+$ (white columns) and CD8$^+$ splenocytes (black columns) as measured by CFSE dilution at day 5 or 3, respectively, of stimulation with anti-CD3/CD28 beads alone (Nihil) or in the presence of irradiated TLN-SCs (1:10 ratio). H, CFSE dilution of CD8$^+$ cells from PDLN of 12-week-old TRAMP and WT mice, which were treated with AMD3100 or vehicle (PBS), at day 3 of stimulation with anti-CD3/CD28 beads. Each panel is representative of at least two independent experiments performed with at least 3 mice per group if not differently indicated. ANOVA followed by the Tukey test and the Student *t* test: *, $P < 0.05$; **, $P < 0.01$; ***, $P < 0.0001$.

We also found that CSC either from mPIN or PDLN of mice affected by mPIN likely overcome immune surveillance by inhibiting T-cell proliferation and effector functions. Several experimental evidences let us conclude that TNC is one major mechanism by which CSCs inhibit T-cell response in TRAMP mice. Indeed, prostate CSC overexpressed TNC and TNC silencing abrogated CSC-mediated immunosuppression. Furthermore, TNC *in vitro* recapitulated the immunosuppressive activity of CSC.

Whereas TNC does not correlate with prostate cancer Gleason score (40), data reported herein in ref. 40 indicate that in normal prostate and low-grade PIN, TNC is weakly expressed in the ECM and acinar basement membrane, its expression increases in high-grade PIN, returns to basal levels in prostate adenocarcinoma, and is again overexpressed in metastases. TNC also is overexpressed in melanoma spheres enriched in CSC, supporting their growth, metastatic potential, and resistance to chemotherapy (41). Accordingly, while TNC was dispensable for TPIN-SC growth *in vitro*, it had a role in supporting their tumor formation *in vivo*. Thus, TNC has a dual role for prostate CSC *in vivo*; on the one hand, it sustains tumor growth, and on the other hand, it inhibits T cell–mediated immune surveillance. TNC is therefore a very interesting target of cancer therapy, and anti-TNC antibodies are already in the clinic (42). It is also tempting to speculate that overexpression of TNC in high-grade PIN and low Gleason score patients, because of the role of TNC in tissue remodeling

and metastasis (26), might identify a subgroup of patients with increased chances of early LN invasion. This hypothesis should be investigated in a large cohort of patients.

CSCs use TNC to block T-cell activation during priming/restimulation, but are ineffective on fully activated T cells, as it has been reported for TNC (27). Hence, CSC do not appear to directly interfere with TCR–MHC interactions, nor TNC interferes with LFA1–ICAM1 interaction (27). It is well known that TNC can bind several molecules among integrins (15). In particular, the fragment FnIII 1–5 of TNC inhibits α5β1-dependent T-cell adhesion to fibronectin (43), while the fragment FnIII A1A2 inhibits T-cell proliferation through a yet unknown mechanism (44). Although we did not investigate which TNC fragment is involved in the CSC-mediated immunosuppressive activity, our *in vitro* findings strongly support a mechanism by which TNC interacts with α5β1 integrins on T-cell surface, thus likely inhibiting Rho activation as previously reported in fibroblasts (30), and blocking actin stress fibers assembly and focal adhesion formation. The signaling cascade triggered by TCR engagement activates Rho, Rac, and Cdc42 GTPases (31). In particular, phosphorylated Zap70 can activate a pathway leading to the formation of a complex of proteins, including VAV1, which facilitates the exchange from GDP to GTP and thus the activation of Rho, Rac, and Cdc42 (32). As TNC inhibits TCR signaling and Zap70 phosphorylation in particular, this could be a complementary mechanism by which TNC inhibit Rho, Rac, and Cdc42 GTPases.

Both CSCs and TNC significantly reduced phosphorylation of ZAP70 and ERK2 and induced substantial metabolic alterations in T cells, as those described in T-cell anergy (24). The state of T-cell hyporesponsiveness induced by TPIN-SCs does not corresponds to the physiologic state of activation-induced nonresponsiveness (45), because T cells lost not only proliferation competence, but also IFNγ production and cytotoxic activity; neither can it be considered as adaptive tolerance, because removal of CSC/TNC allowed full T-cell recovery. Thus, the effect mediated by CSC on T cells is characteristic more of cell-mediated immunosuppression (24).

Silencing of TNC did not completely abrogate the immunosuppressive activity of CSC and did not rescue STAT5 phosphorylation, suggesting that other molecules are involved in CSC-mediated immunosuppression. Indeed, microarray-based whole transcript showed that both TPIN-SC and TLN-SC produce several other immunomodulatory factors, currently investigated by us.

Peripheral tolerance to tumor-associated antigens in prostate cancer may be induced and maintained by several additional mechanisms. Indeed, CSC and/or other more differentiated tumor cells may generate immunosuppressive networks within the primary lesion, and anergic Tag-specific $CD8^+$ T cells are found in the prostate of TRAMP mice (14). Both regulatory T cells and myeloid-derived suppressor cells accumulate in the prostate of cancer patients and TRAMP mice, although their targeting revealed insufficient for breaking T-cell tolerance and sustaining antitumor immunity (46, 47). Moreover, in TRAMP and in human prostate cancer lesions, a population of tolerogenic DCs induces $CD8^+$ T cells to acquire suppressive functions through indoleamine-2,3-dioxygenase, arginase, TGFβ, and PDL-1 (48).

Our results merge the evidence of early tumor cell dissemination with tumor-induced immune escape, with relevant clinical implications. In our cohort, TRAMP mice never developed LN metastasis from prostate adenocarcinoma before week 17 (data not shown), suggesting that CSC that have colonized PDLN remain quiescent for several weeks. Immune surveillance appears to be involved in limiting the metastatic outgrowth, as cytostatic $CD8^+$ T cells have been shown to maintain DTC dormancy in visceral organs (49). Thus, strategies that either block the interaction between TNC and α5β1, such as antibodies (42) or isoGDR peptides, or the CXCR4–CXL12 axis (50), as the one described herein, or both TNC and CXCR4 should unsheathe early-disseminated CSC and avoid full-blown metastasis development, and might be proposed either alone or in combination to subjects with high risk to develop prostate cancer or to patients at high risk for disease recurrence after radical prostatectomy. Although in our cohort of TRAMP mice, the earliest metastasis from adenocarcinoma was found in the kidney at 16 weeks of age, metastasis to soft tissues in this model is rather infrequent and stochastic. Hence, efficacy of the proposed treatments in preventing metastasis occurrence to soft tissues might better be investigated in other models.

Disclosure of Potential Conflicts of Interest

No potential conflicts of interest were disclosed.

Authors' Contributions

Conception and design: E. Jachetti, S. Caputo, A. Calcinotto, M. Bellone
Development of methodology: E. Jachetti, S. Caputo, S.M. Parigi, A. Calcinotto, A. Bachi
Acquisition of data (provided animals, acquired and managed patients, provided facilities, etc.): E. Jachetti, S. Caputo, C.S. Brambillasca, S.M. Parigi, M. Grioni, U. Restuccia, A. Calcinotto, M. Freschi, A. Bachi
Analysis and interpretation of data (e.g., statistical analysis, biostatistics, computational analysis): E. Jachetti, S. Caputo, C.S. Brambillasca, S.M. Parigi, I.S. Piras, U. Restuccia, M. Freschi, A. Bachi, M. Bellone
Writing, review, and/or revision of the manuscript: E. Jachetti, S. Caputo, U. Restuccia, M. Freschi, A. Bachi, M. Bellone
Administrative, technical, or material support (i.e., reporting or organizing data, constructing databases): E. Jachetti, M. Grioni
Study supervision: E. Jachetti, R. Galli, M. Bellone
Other (prostate cancer stem cell lines establishment and characterization): S. Mazzoleni

Acknowledgments

The authors thank Drs. A. Mondino, M.P. Protti, R. Pardi, I. De Curtis, A. Corti, and F. Curnis (San Raffaele Scientific Institute, Milan, Italy) and R. Longhi (Consiglio Nazionale Ricerche, Milan, Italy) for critical comments, helpful suggestions, and reagents, and Dr. S. Scala (Fondazione Pascale, Napoli, Italy) for Peptide R.

Grant Support

The work was supported by Associazione Italiana per la Ricerca sul Cancro (AIRC; # IG11692) and Ministero della Salute. E. Jachetti and A. Calcinotto were awarded an AIRC/FIRC fellowship. S. Caputo and A. Calcinotto conducted this study in partial fulfillment of their Ph.D. at San Raffaele University.

The costs of publication of this article were defrayed in part by the payment of page charges. This article must therefore be hereby marked *advertisement* in accordance with 18 U.S.C. Section 1734 solely to indicate this fact.

Received August 12, 2014; revised January 31, 2015; accepted February 23, 2015; published OnlineFirst March 25, 2015.

References

1. Klein CA. Parallel progression of primary tumours and metastases. Nat Rev Cancer 2009;9:302–12.
2. Husemann Y, Geigl JB, Schubert F, Musiani P, Meyer M, Burghart E, et al. Systemic spread is an early step in breast cancer. Cancer Cell 2008;13:58–68.
3. Visvader JE, Lindeman GJ. Cancer stem cells in solid tumours: accumulating evidence and unresolved questions. Nat Rev Cancer 2008;8:755–68.
4. Hermann PC, Huber SL, Herrler T, Aicher A, Ellwart JW, Guba M, et al. Distinct populations of cancer stem cells determine tumor growth and metastatic activity in human pancreatic cancer. Cell Stem Cell 2007;1:313–23.
5. Rhim AD, Mirek ET, Aiello NM, Maitra A, Bailey JM, McAllister F, et al. EMT and dissemination precede pancreatic tumor formation. Cell 2012;148:349–61.
6. Aguirre-Ghiso JA. Models, mechanisms and clinical evidence for cancer dormancy. Nat Rev Cancer 2007;7:834–46.
7. Brown CE, Starr R, Martinez C, Aguilar B, D'Apuzzo M, Todorov I, et al. Recognition and killing of brain tumor stem-like initiating cells by $CD8^+$ cytolytic T cells. Cancer Res 2009;69:8886–93.
8. Castriconi R, Daga A, Dondero A, Zona G, Poliani PL, Melotti A, et al. NK cells recognize and kill human glioblastoma cells with stem cell-like properties. J Immunol 2009;182:3530–9.
9. Wei J, Barr J, Kong LY, Wang Y, Wu A, Sharma AK, et al. Glioma-associated cancer-initiating cells induce immunosuppression. Clin Cancer Res 2010;16:461–73.
10. Greenberg NM, DeMayo F, Finegold MJ, Medina D, Tilley WD, Aspinall JO, et al. Prostate cancer in a transgenic mouse. Proc Natl Acad Sci U S A 1995;92:3439–43.
11. Shappell SB, Thomas GV, Roberts RL, Herbert R, Ittmann MM, Rubin MA, et al. Prostate pathology of genetically engineered mice: definitions and classification. The consensus report from the Bar Harbor meeting of the Mouse Models of Human Cancer Consortium Prostate Pathology Committee. Cancer Res 2004;64:2270–305.
12. Mazzoleni S, Jachetti E, Morosini S, Grioni M, Piras IS, Pala M, et al. Gene signatures distinguish stage-specific prostate cancer stem cells from transgenic adenocarcinoma of the mouse prostate (TRAMP) lesions and predict the malignancy of human tumors. Stem Cells Trans Med 2013;2:678–89.
13. Jachetti E, Mazzoleni S, Grioni M, Ricupito A, Brambillasca C, Generoso L, et al. Prostate cancer stem cells are targets of both innate and adaptive immunity and elicit tumor-specific immune responses. Oncoimmunology 2013;2:e24520.
14. Degl'Innocenti E, Grioni M, Boni A, Camporeale A, Bertilaccio MT, Freschi M, et al. Peripheral T cell tolerance occurs early during spontaneous prostate cancer development and can be rescued by dendritic cell immunization. Eur J Immunol 2005;35:66–75.
15. Orend G, Chiquet-Ehrismann R. Tenascin-C induced signaling in cancer. Cancer Lett 2006;244:143–63.
16. Mombaerts P, Iacomini J, Johnson RS, Herrup K, Tonegawa S, Papaioannou VE. RAG-1-deficient mice have no mature B and T lymphocytes. Cell 1992;68:869–77.
17. Bellone M, Cantarella D, Castiglioni P, Crosti MC, Ronchetti A, Moro M, et al. Relevance of the tumor antigen in the validation of three vaccination strategies for melanoma. J Immunol 2000;165:2651–6.
18. Curnis F, Sacchi A, Longhi R, Colombo B, Gasparri A, Corti A. IsoDGR-tagged albumin: a new alphavbeta3 selective carrier for nanodrug delivery to tumors. Small 2013;9:673–8.
19. Restuccia U, Boschetti E, Fasoli E, Fortis F, Guerrier L, Bachi A, et al. pI-based fractionation of serum proteomes versus anion exchange after enhancement of low-abundance proteins by means of peptide libraries. J Proteomics 2009;72:1061–70.
20. Olsen JV, de Godoy LM, Li G, Macek B, Mortensen P, Pesch R, et al. Parts per million mass accuracy on an Orbitrap mass spectrometer via lock mass injection into a C-trap. Mol Cell Proteomics 2005;4:2010–21.
21. Groom JR, Richmond J, Murooka TT, Sorensen EW, Sung JH, Bankert K, et al. CXCR3 chemokine receptor-ligand interactions in the lymph node optimize $CD4^+$ T helper 1 cell differentiation. Immunity 2012;37:1091–103.
22. Hogquist KA, Jameson SC, Heath WR, Howard JL, Bevan MJ, Carbone FR. T cell receptor antagonist peptides induce positive selection. Cell 1994;76:17–27.
23. Barnden MJ, Allison J, Heath WR, Carbone FR. Defective TCR expression in transgenic mice constructed using cDNA-based alpha- and beta-chain genes under the control of heterologous regulatory elements. Immunol Cell Biol 1998;76:34–40.
24. Schwartz RH. T cell anergy. Annu Rev Immunol 2003;21:305–34.
25. MacIver NJ, Michalek RD, Rathmell JC. Metabolic regulation of T lymphocytes. Annu Rev Immunol 2013;31:259–83.
26. Oskarsson T, Acharyya S, Zhang XH, Vanharanta S, Tavazoie SF, Morris PG, et al. Breast cancer cells produce tenascin C as a metastatic niche component to colonize the lungs. Nat Med 2011;17:867–74.
27. Ruegg CR, Chiquet-Ehrismann R, Alkan SS. Tenascin, an extracellular matrix protein, exerts immunomodulatory activities. Proc Natl Acad Sci U S A 1989;86:7437–41.
28. Nobes CD, Hall A. Rho, rac, and cdc42 GTPases regulate the assembly of multimolecular focal complexes associated with actin stress fibers, lamellipodia, and filopodia. Cell 1995;81:53–62.
29. Woodside DG, Wooten DK, McIntyre BW. Adenosine diphosphate (ADP)-ribosylation of the guanosine triphosphatase (GTPase) rho in resting peripheral blood human T lymphocytes results in pseudopodial extension and the inhibition of T cell activation. J Exp Med 1998;188:1211–21.
30. Wenk MB, Midwood KS, Schwarzbauer JE. Tenascin-C suppresses Rho activation. J Cell Biol 2000;150:913–20.
31. Rougerie P, Delon J. Rho GTPases: masters of T lymphocyte migration and activation. Immunol Lett 2012;142:1–13.
32. Tybulewicz VL, Henderson RB. Rho family GTPases and their regulators in lymphocytes. Nat Rev Immunol 2009;9:630–44.
33. Feller SM. Crk family adaptors-signalling complex formation and biological roles. Oncogene 2001;20:6348–71.
34. Rich S, Van Nood N, Lee HM. Role of alpha 5 beta 1 integrin in TGF-beta 1-costimulated CD8+ T cell growth and apoptosis. J Immunol 1996;157:2916–23.
35. Portella L, Vitale R, De Luca S, D'Alterio C, Ierano C, Napolitano M, et al. Preclinical development of a novel class of CXCR4 antagonist impairing solid tumors growth and metastases. PLoS ONE 2013;8:e74548.
36. Jiao J, Hindoyan A, Wang S, Tran LM, Goldstein AS, Lawson D, et al. Identification of CD166 as a surface marker for enriching prostate stem/progenitor and cancer initiating cells. PLoS ONE 2012;7:e42564.
37. Hubert RS, Vivanco I, Chen E, Rastegar S, Leong K, Mitchell SC, et al. STEAP: a prostate-specific cell-surface antigen highly expressed in human prostate tumors. Proc Natl Acad Sci U S A 1999;96:14523–8.
38. Reiter RE, Gu Z, Watabe T, Thomas G, Szigeti K, Davis E, et al. Prostate stem cell antigen: a cell surface marker overexpressed in prostate cancer. Proc Natl Acad Sci U S A 1998;95:1735–40.
39. Pagliarulo V, Hawes D, Brands FH, Groshen S, Cai J, Stein JP, et al. Detection of occult lymph node metastases in locally advanced node-negative prostate cancer. J Clin Oncol 2006;24:2735–42.
40. Slater MD, Lauer C, Gidley-Baird A, Barden JA. Markers for the development of early prostate cancer. J Pathol 2003;199:368–77.
41. Fukunaga-Kalabis M, Martinez G, Nguyen TK, Kim D, Santiago-Walker A, Roesch A, et al. Tenascin-C promotes melanoma progression by maintaining the ABCB5-positive side population. Oncogene 2010;29:6115–24.
42. Rizzieri DA, Akabani G, Zalutsky MR, Coleman RE, Metzler SD, Bowsher JE, et al. Phase 1 trial study of 131I-labeled chimeric 81C6 monoclonal antibody for the treatment of patients with non-Hodgkin lymphoma. Blood 2004;104:642–8.
43. Hauzenberger D, Olivier P, Gundersen D, Ruegg C. Tenascin-C inhibits beta1 integrin-dependent T lymphocyte adhesion to fibronectin through the binding of its fnIII 1–5 repeats to fibronectin. Eur J Immunol 1999;29:1435–47.
44. Puente Navazo MD, Valmori D, Ruegg C. The alternatively spliced domain TnFnIII A1A2 of the extracellular matrix protein tenascin-C suppresses activation-induced T lymphocyte proliferation and cytokine production. J Immunol 2001;167:6431–40.
45. Mescher MF, Popescu FE, Gerner M, Hammerbeck CD, Curtsinger JM. Activation-induced non-responsiveness (anergy) limits CD8 T cell responses to tumors. Semin Cancer Biol 2007;17:299–308.
46. Degl'Innocenti E, Grioni M, Capuano G, Jachetti E, Freschi M, Bertilaccio MT, et al. Peripheral T-cell tolerance associated with prostate cancer is independent from $CD4^+CD25^+$ regulatory T cells. Cancer Res 2008;68:292–300.

47. Rigamonti N, Capuano G, Ricupito A, Jachetti E, Grioni M, Generoso L, et al. Modulators of arginine metabolism do not impact on peripheral T-cell tolerance and disease progression in a model of spontaneous prostate cancer. Clin Cancer Res 2011;17:1012–23.
48. Watkins SK, Zhu Z, Riboldi E, Shafer-Weaver KA, Stagliano KE, Sklavos MM, et al. FOXO3 programs tumor-associated DCs to become tolerogenic in human and murine prostate cancer. J Clin Invest 2011;121: 1361–72.
49. Eyles J, Puaux AL, Wang X, Toh B, Prakash C, Hong M, et al. Tumor cells disseminate early, but immunosurveillance limits metastatic outgrowth, in a mouse model of melanoma. J Clin Invest 2010;120: 2030–9.
50. Shanmugam MK, Manu KA, Ong TH, Ramachandran L, Surana R, Bist P, et al. Inhibition of CXCR4/CXCL12 signaling axis by ursolic acid leads to suppression of metastasis in transgenic adenocarcinoma of mouse prostate model. Int J Cancer 2011;129:1552–63.